Synthetic strategies for modifying dielectric properties and the electron mobility of fullerene derivatives

Jahani Bahnamiri, Fatemeh

Chapter 3

Increasing the Dielectric Constant of Fullerene Derivatives by TEG Side-chains

Abstract

Development of new organic materials with high dielectric constant is crucial for the development of organic-based devices such as organic solar cells. In this chapter a synthetic way is proposed to increase the dielectric constant of fullerene derivatives. It is demonstrated that introducing triethylene glycol monoethyl ether (TEG) side chains to fulleropyrrolidines increases the dielectric constant by $\sim$ 46 percent without devaluation of optical properties, electron mobility, and orbital energy levels of the compound.

Part of the work described in this chapter was done in cooperation with S. Torabi, Dr. L.J.A. Koster and Dr. R.W.A. Havenith. Part of this work was published in Chem. Commun. 2014 (vol. 50, p. 10645-10647) and Adv. Funct. Mater. 2015 (vol. 25, p. 150-157).

3.1 Introduction

The dielectric properties of molecular materials are crucial to a host of important phenomena, including enzyme function [1], electron transfer [2, 3], chemical sensors [4, 5] and a variety of electronic applications [6, 7] such as in self-assembled nano-scale dielectric materials for gating thin-film transistors [8–10] as well as in thin interfacial extraction/blocking layers for organic light-emitting diodes and photovoltaic cells [11–15]. Yet, there are no common synthetic tools for affecting dielectric properties as there are, for example, for tuning band gaps, hydrophobicity, etc.

We are particularly interested in π-conjugated organic materials with high dielectric constant (ε_r) for applications in organic photovoltaics (OPV). In a recent theoretical study, we showed that increasing ε_r reduces the exciton binding energy and recombination losses, making organic solar cells with power conversion efficiencies above 20% feasible [16]. Therefore, tailoring organic materials for enhanced ε_r is a viable route for efficiency enhancement of current OPV systems. This will potentially benefit other applications of organic semiconductors that currently suffer from their poor dielectric properties. In a more ambitious perspective, the enhancement of dielectric constant for organic materials results into a reduction of the exciton binding energy, which can effectively rule out the need for the bulk heterojunction structures, directing the progressive pathway of OPV to a new milestone [16].

To date, little focus has been devoted to improving dielectric constants in conjugated organic materials; there are only few examples of ε_r greater than 3-4 in these materials. As mentioned earlier in the introduction chapter, incorporation of polar groups into the molecular structure of the material is a possible way for increasing the dielectric constant. Although there is nothing inherently wrong with the general strategy of installing polar pendant groups, a generalizable route to prepare high dielectric constant π-conjugated organic materials has proven elusive; e.g., what constitutes a polarizable pendant group and how strongly does it influence the properties of a conjugated material?

Breselge et al [17] introduced triethylene glycol (TEG) side chains in a poly(p-phenylene vinylene) (PPV) derivative and showed an enhancement of the dielectric constant. When blended with a fullerene derivative, this polymer yielded enhanced charge dissociation compared to less polar PPV derivatives [18]. However, the BHJ solar cell did not present efficiency enhancement, reportedly due to the incompatible polarities of the polymer and PCBM leading to the formation of large domains in the donor-acceptor network [17]. Therefore, in order to provide

better mixing for the donor-acceptor blend, it is beneficial to functionalize both components with almost identical polarities.
Although much research focuses on modifying the electronic, optical, and solubility properties of fullerene derivatives, increasing the polarizability and hence ε_r without sacrificing these properties is an important challenge in organic solar cell materials that has not yet been solved.

3.1.1 Research goals

Fullerene derivatives are known as very efficient acceptors in OPV and show excellent electron transport properties [19]. In order to enhance the polarity and dielectric constant, polarizable triethylene glycol ethyl ether (TEG) side chains were added to C_{60}, to obtain the fullerene derivatives, dubbed PTEG-1 and PTEG-2. To differentiate the role of TEG on the dielectric constant of fullerene derivatives, an analogous fullerene derivative (PP) without TEG side chains was synthesized.

3.2 DFT calculations

Molecular dynamic studies on poly(ethylene glycol) (PEG) have confirmed their high chain flexibility and rapid motion of polar components [20]. Ethylene glycol and triethylene glycol yield dielectric constant values in the range of 5-40 in the liquid phase at drive frequencies of 1-20 GHz [21]. Havenith recently investigated this phenomenon with us on a molecular scale in a theoretical study. According to density functional theory (DFT) calculations (B3LYP/6-31G**) applied for a model TEG chain (see Figure 3.1), using GAMESS-UK [22] rotation around the H_2C-CH_2 and H_2C-O bonds can be very fast at room temperature.

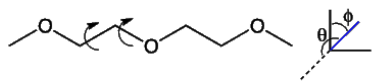

Figure 3.1: Repeating units of EG. Indicated are the rotations around the H_2C-CH_2 and H_2C-O bonds, and the axes of the direction of the dipole moment with respect to the molecule (θ, ϕ).

The rotational profiles around these bonds show two low barriers of ~ 0.11 and ~ 0.08 eV for H_2C-CH_2 and H_2C-O rotations and larger barriers of ~ 0.35 and ~ 0.29 eV, respectively (Figure

3.2). The activation energy of 0.11 eV corresponds to a reaction rate of 0.95×10^9 s^{-1} at 175K according to equation 3.1 [23].

$$k_{rate} = \frac{k_b T}{h} \exp(-\frac{\Delta G}{RT}) \tag{3.1}$$

where k_{rate} is the reaction rate, k_b, h and R are Boltzmann, Planck and gas constants respectively, T is the temperature and ΔG is the Gibbs free energy difference. Thus the rotation of angles ϕ between $\sim 75°$ and $\sim 285°$ of all bonds occurs readily at low temperatures. Full rotation is still active at 175K to overcome the barrier of 0.35 eV. The reaction rates of 1.7×10^{11} s^{-1} and 1.7×10^7 s^{-1} correspond to the activation energies of 0.11 eV and 0.35 eV respectively at 298K. Hence, at room temperature, rotations of ϕ between $\sim 75°$ and $\sim 285°$ are active in GHz frequency-domain and full rotation in MHz range occurs readily. During these rotations, the magnitude of the dipole moment barely changes, but the direction of this dipole moment changes considerably (b,c).

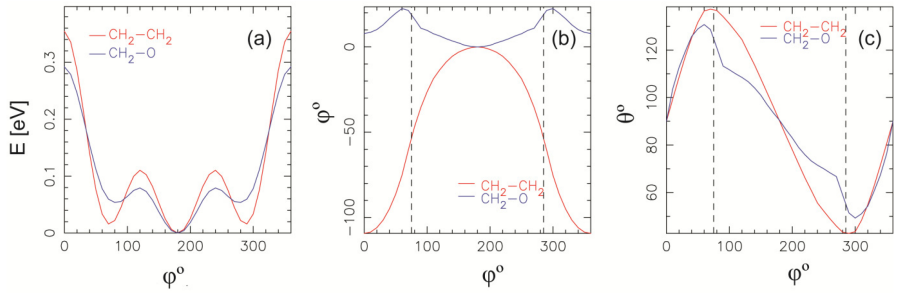

Figure 3.2: a) The energy with respect to the minimum as a function of the dihedral angle of the H_2C-CH_2 and H_2C-O bonds, b) the angle θ of the dipole moment as a function of the dihedral angle of the H_2C-CH_2 and H_2C-O bonds, and c) the angle ϕ of the dipole moment as a function of the dihedral angle of the H_2C-CH_2 and H_2C-O bonds.

The swiftness and flexibility of TEG chains can provide easier reorientations for dipole moments, and thus potentially increase dielectric constant when being added to fullerenes in the GHz range.

3.3 Synthesis

Fullerenes in general are widely utilized as acceptors and phenyl-C_{61}-butyric acid methyl ester (PCBM) is the most widely used fullerene acceptor in OPV devices. Fulleropyrrolidines are easily prepared via the Prato method [24], a 1,3-dipolar cycloaddition of an azomethine ylide, generated in situ from the corresponding aldehyde and *N*-methylglycine. This methodology has proven to be a powerful procedure for the functionalization of C_{60} due to its versatility and the availability of the starting materials, while making methano[60]fullerenes has some limitations in terms of molecule design and method. For instance the preparation of ylides and, in particular diazo compounds, can be difficult.

The synthetic route to prepare PTEG-1, PTEG-2 and PP is shown in Scheme 3.1. Treatment of triethylene glycol monoethyl ether (1) with toluene-*p*-sulfonyl chloride (TsCl) and NaOH, followed by a Williamson-type reaction of the resulting tosylate (2) with *p*-hydroxybenzaldehyde in the presence of K_2CO_3 in DMF at 90°C afforded corresponding benzaldehyde (3). The target fulleropyrrolidine (PTEG-1) (4) was prepared by 1,3-dipolar cycloaddition of the aldehyde (3), *N*-methylglycine and C_{60} according to the Prato method in ODCB at 90 °C in 39% yield. PTEG-2 (6) was synthesized from 3,5-dihydroxybenzaldehyde by following a similar synthetic approach as described above in 32% yield. For comparison, we also prepared PP (8), which lacks TEG chains, starting from benzaldehyde.

3.4 Characterization

The structures of the synthesized compounds were confirmed by analytical and spectroscopic data. The ^{1}H-NMR spectra of PTEG-1 and PTEG-2, recorded in $CDCl_3$, exhibit the expected signals of a TEG moiety and the characteristic peaks of the pyrrolidine ring as two doublets (AB quartet) and one singlet as well as a singlet for the N-CH_3 group. In fulleropyrrolidines the signals of the ortho-hydrogen atoms of the phenyl group directly attached to the pyrrolidine ring appear as broad singlet at room temperature due to restricted rotation of phenyl group.

3.4.1 UV-vis absorption measurement

Figure 3.3 shows the UV-vis absorption spectra of compounds PTEG-1 and PTEG-2 together with that of reference compound PP in 10^{-5} M $CHCl_3$. C_{60} derivatives generally display strong

Scheme 3.1: Synthetic rout for preparing PTEG-1, PTEG-2 and PP as the reference compound.

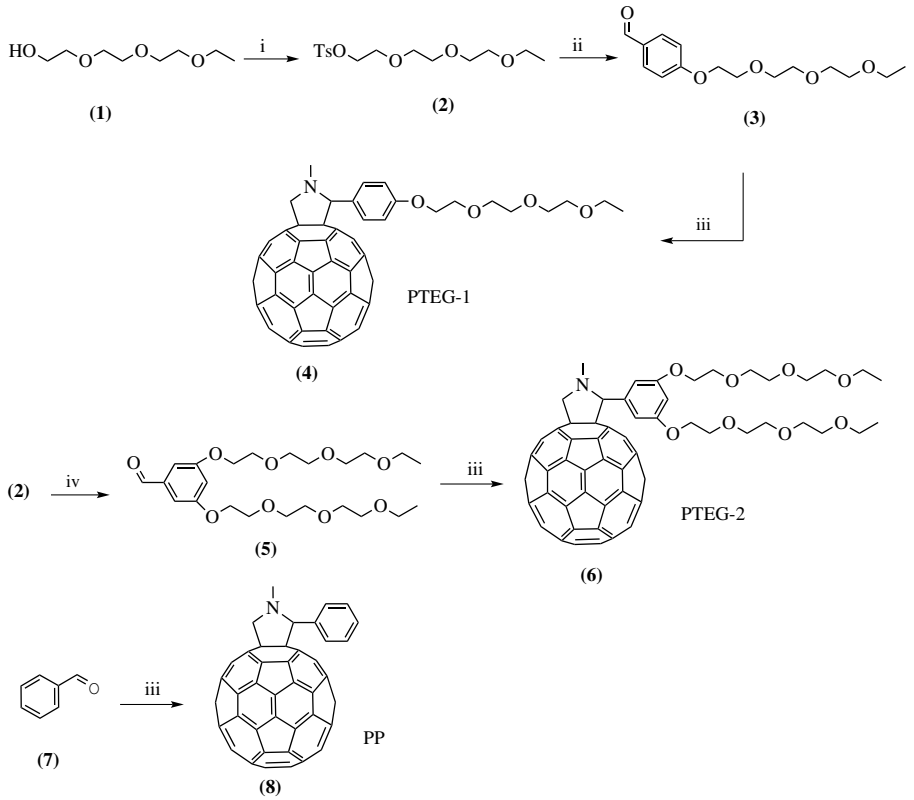

i) TsCl, NaOH, THF, ii) 4-hydroxybenzaldehyde, K_2CO_3, DMF, iii) C_{60}, sarcosine, ODCB, 90 ^oC,
iv) 3,5-dihydroxybenzaldehyde, K_2CO_3, DMF

absorption in the UV region and broad, weak absorption in visible region. The absorption of PTEG-1 and PTEG-2 is almost the same as PP, especially the characteristic peak of the fullerene moiety at 430 and 704 nm. This similarity indicates that TEG chains do not have any significant effect on UV-vis absorption, hence no electronic interaction with the fullerene cage, in $CHCl_3$.

3.4.2 Cyclic voltammetry measurement

The electrochemistry of fullerenes is one of their most important properties as conjugated materials for use in OPV. Therefore, we investigated the electrochemical properties of PTEG-1 and PTEG-2 by cyclic voltammetry. We also studied PP for comparison (see Figure 3.4). The mea-

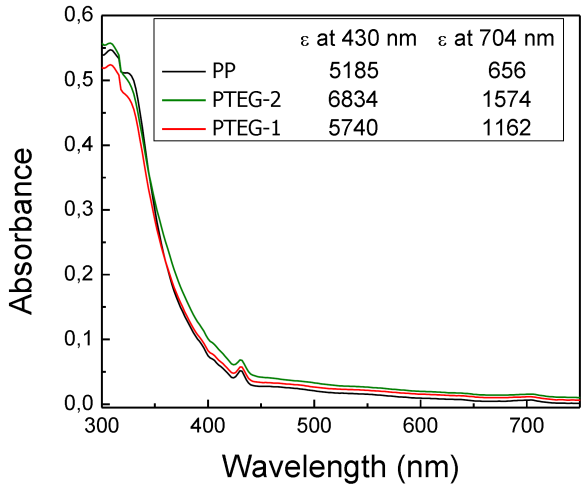

Figure 3.3: UV-vis absorption spectra of PTEG-1, PTEG-2 and PP in 10^{-5} M $CHCl_3$ solution.

sured half-wave potentials of the first two reduction processes of all compounds are listed in Table 3.1. The first reduction potential, which approximates the LUMO energy level of these compounds, is almost the same for PTEG-1, PTEG-2, and the controls compounds, PP and PCBM. This similarity implies that TEG chains do not affect the LUMO energy of fullerene derivatives (because they do not shift the reduction potentials) under these circumstances. In addition, there is no significant change in the potential of the second reduction.

Table 3.1: Electrochemical properties of PTEG-1, PTEG-2, PP and PCBM.

Compound	$E_{1/2}$ 1, red [a]	$E_{1/2}$ 2, red [a]
PCBM	-1.092	-1.482
PTEG-1	-1.113	-1.511
PTEG-2	-1.106	-1.504
PP	-1.114	-1.508

[a] V vs Fc/Fc^+

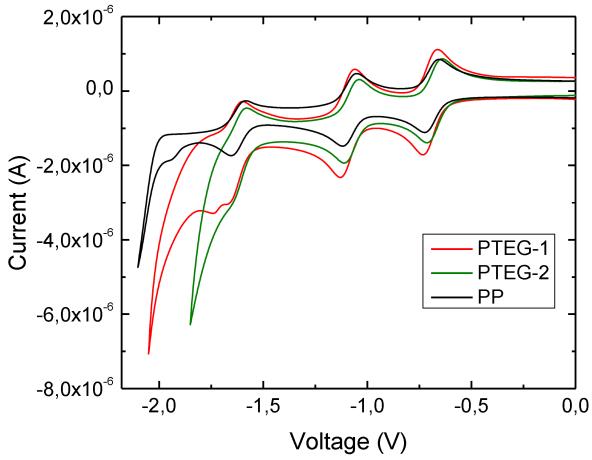

Figure 3.4: Cyclic voltammograms of PTEG-1, PTEG-2 and PP; experimental conditions: Bu_4NPF_6 (0.1 M) as the supporting electrolyte, ODCB/CH_3CN (4:1) as solvent; Pt, working electrode; Pt wire, counter electrode; Ag/AgCl, reference electrode; scan rate 10 mV/s, Fc/Fc^+ as internal standard.

3.5 Solubility of fullerene derivatives with TEG side chains

A notable feature of the fulleropyrrolidine, PTEG-1, is its improved solubility compared to PCBM in wide range of common organic solvents such as o-dichlorobenzene (ODCB), PhCl, $CHCl_3$, dichloromethane (DCM), toluene and THF. For example, PCBM is reasonably soluble in $CHCl_3$ (∼25 mg/ml), ODCB (∼ 30 mg/ml) and toluene (10 mg/ml), but much less soluble in THF, while PTEG-1 is easily dissolved in ODCB (∼ 65 mg/ml), $CHCl_3$ (∼ 45 mg/ml), toluene (∼ 36 mg/ml) and THF (∼ 15 mg/ml). This enhancement of solubility is not only an important issue for the fabrication of layers in electronic devices, but also opens the possibility of using sustainable and/or less harmful solvents. PTEG-2, with two TEG chains, shows even better solubility in organic solvents. Importantly, this increased solubility did not impact any electronic properties.

3.6 Dielectric constant of fulleropyrrolidines with TEG side chains

It is well known that, as polarizability increases the dielectric constant increases, and the more available polarization mechanisms a material possesses, the larger the dielectric constant can be expected. According to DFT calculation, we expect the addition of TEG chain(s) to fullerenes to increase the relative permittivity of fullerene compound by increasing the mechanisms of polarization via the reorientation of the dipole moments of the ethers in TEG.

Table 3.2: Relative dielectric constant of PTEG-1, PTEG-2 and PP.

Fullerene derivatives	ε_r	tested capacitors #
PP	3.8 ± 0.4	12
PTEG-1	5.7 ± 0.2	6
PTEG-2	5.3 ± 0.2	4

Table 3.2 lists dielectric constant values of all the synthesized materials, determined via spectral impedance measurements in the frequency range of 100 Hz to 1MHz (for details regarding the dielectric constant measurement the reader is referred to section 2.6.2 of chapter 2). Interestingly, the dielectric constant for both PTEG-1 and PTEG-2 increased significantly to 5.7 and 5.3 respectively, in comparison to PP ($\varepsilon_r \sim 3.8$) and PCBM ($\varepsilon_r \sim 3.9$). The determined dielectric constant for all three compounds is constant from 100 to 10^6 Hz. This enhancement of the dielectric properties clearly shows the influence of the increased polarizability afforded by TEG side chains.

In general, the fast change in the direction of the dipole moment can account for the high ε_r of materials with incorporated ethylene glycol chains. Figure 3.5 depicts determined dielectric constant versus frequency for PTEG-1, PTEG-2 and PP. As is clear from the DFT calculations in section 3.2, the reaction rate for the change in the dipole moment direction is strongly temperature dependent for a model TEG chain. To test the validity of these calculations experimentally, the temperature dependence of ε_r was studied for TEG-functionalized compounds. As can be seen from Figure 3.6, dielectric constant of PTEG-2 is temperature dependent. However, the temperature dependence for PTEG-1 is not detectable, similar to that of its reference com-

pound. At present, we do not understand the reason for this difference in behavior. We can only speculate that this might be due to the presence of steric effects in the solid state, such as different molecular packing influencing the dipole moment alignments.

The measured dielectric constants of PTEG-1 and PTEG-2 differ only by the sum of their standard deviations. This observation might seem counterintuitive, because one might expect that two highly polar TEG moieties per molecule would have a greater influence than one. We therefore tentatively conclude that the measured permittivity results from a complex interplay between the fullerene cages and their substituents and is not simply a result of increasing the volume fraction of glycol units in the film. This situation is quite different from that of the addition of macroscopic high-ε fillers.

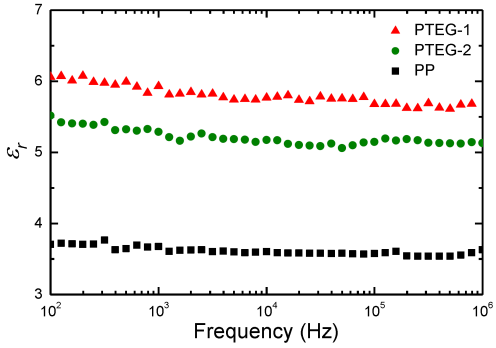

Figure 3.5: Dielectric constant versus frequency at room temperature for PTEG-1, PTEG-2 and PP.

3.7 Charge carrier mobility of fulleropyrrolidine with TEG side chains

We investigated the electron mobility of films of the fullerene derivatives by measuring the current-voltage characteristics of electron-only devices with the following architecture at room temperature: Au/fullerene derivative/LiF/Al (for details regarding the electron mobility measurement the reader is referred to section 2.6.3 of chapter 2). The experimental J-V curves show that current density quadratically depends on the voltage, in the range above the built-in voltage V_{bi}, which is a characteristic behavior for space-charge limited current (SCLC) [25]. The

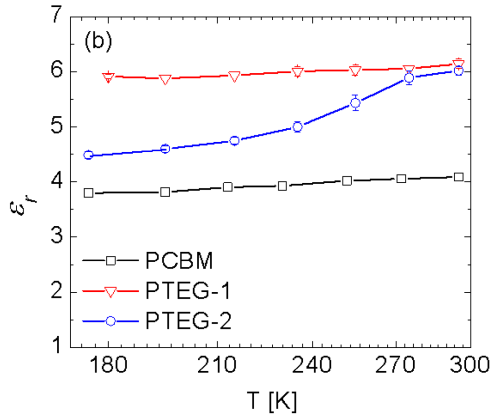

Figure 3.6: Temperature dependence of the relative dielectric constant for PTEG-1 and PTEG-2 compared with PCBM. The lines are guides to the eye.

J-V curves of PTEG-1 and PTEG-2 are shown in the Figure 3.7 corrected for built-in voltage of $V_{bi} = 0.5$ V and 0.05 V, respectively.

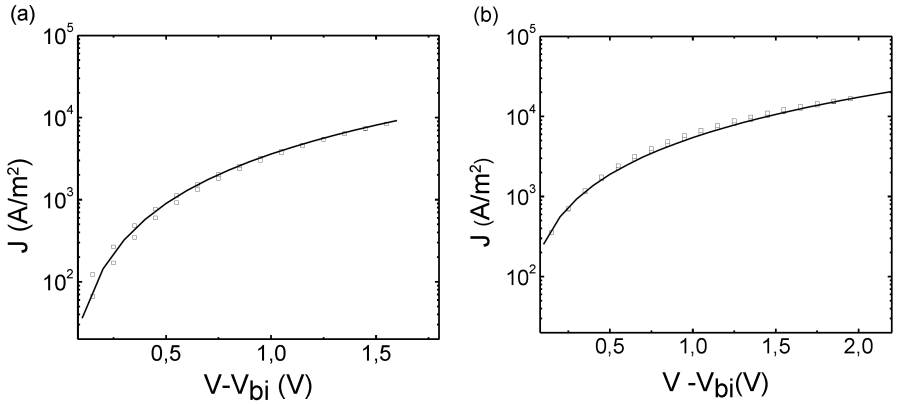

Figure 3.7: Current density versus voltage corrected for (a) $V_{bi} = 0.5$ of Au /PTEG-1/LiF/Al and (b) $V_{bi} = 0.05$ of Al /PTEG-2/Al at room temperatures 295K. Experimental data (symbols) are fitted with SCLC current (solid lines).

We found similar values for the electron mobility of the fullerenes with single and double TEG side chains (PTEG-1 and PTEG-2), PCBM of $\sim 2 \times 10^{-7}$ m^2/Vs (see Table 3.3). Thus, in addition to the electro-optical properties of the molecules being unaffected by inclusion of TEG chains,

their bulk electron mobility did not change with respect to that of the benchmark fullerene derivative, PCBM.

Table 3.3: Electron mobility (μ_e) of PTEG-1, PTEG-2, PP and PCBM.

Compound	$\mu_e[\mathrm{m}^2/\mathrm{Vs}]$
PCBM	2×10^{-7}
PTEG-1	2×10^{-7}
PTEG-2	3.5×10^{-7}
PP	-[a]

[a] Insufficient film quality.

3.8 Conclusions

In conclusion, we synthesized fullerene derivatives with dielectric constants significantly higher than those of C_{60} and PCBM, without negatively impacting their molecular properties (optical absorption and reduction potentials) as well as bulk properties (electron mobility). Our strategy of increasing polarizability by including TEG chains also improved the solubility compared to PCBM in a wide range of organic solvents. This work is one of the first efforts unambiguously demonstrating a synthetic route for orthogonal tuning of the dielectric constant (a bulk property) of a thin film of π-conjugated organic molecules. This orthogonality is critical to the tailoring of high-dielectric-constant materials because it precludes the need to balance the negative impacts of simpler strategies such as the inclusion of additives and the re-optimization of each combination of material/additive. While there are scattered reports of small increases in the dielectric constant of conjugated polymers through the inclusion of polar pendant groups, the strategy presented in this paper opens up new opportunities to improve the power conversion efficiencies of heterojunction OPV devices without perturbing HOMO/LUMO energies or electron mobility of fullerene acceptors. Ultimately this strategy of synthetically manipulating the dielectric properties of materials may lead to single-component, non-excitonic OPV devices.

3.9 Experimental

All reagents and solvents were used as received. All reactions were performed under a nitrogen atmosphere using oven dried glassware (150 °C). The C_{60} used for the syntheses was 99.5% (purchased from Solenne BV, Groningen, The Netherlands). Column chromatography was performed using silica gel (Kieselgel Merck Type 9385, 230-400 mesh). ^{1}H-NMR and ^{13}C-NMR were performed on a Varian Unity Plus (500 MHz) or on a Varian Unity Plus (400 MHz) instrument, as indicated, at 25 °C; Values are reported in ppm; Multiplicities are denoted as follows: s=singlet, m=multiplet, br=broad and J values are given in Hz. IR measurements were performed on a Nicolet Nexus FT-IR instrument. HPLC analyses were performed on an LC-MS system (Agilent/HP 1100 series) using an analytical Cosmosil Buckyprep®column (4.6×250 mm); UV-vis absorption spectra were measured with a Perkin-Elmer Lambda 900 spectrometer.

3.9.1 Synthesis

2-[2-(2-ethoxyethoxy) ethoxy]ethyl *p*-tosylate: [26]

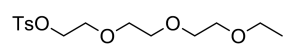

Sodium hydroxide (800 mg, 20 mmol) dissolved in water (4 mL) and 2-[2-(2-ethoxyethoxy) ethoxy]ethanol (2.49 g, 14 mmol) in THF (4mL) were placed in a three-necked, 50 mL flask. The mixture was cooled on an ice bath. *p*-Toluenesulfonyl chloride (2.44 g, 13 mmol) in THF (4 mL) was added drop-wise to the mixture over 1 h. The solution was stirred at 0°C for an additional 3h., then poured into ice-water (150 mL) and extracted with ethyl acetate. The organic layer was washed with water and dried over Na_2SO_4. The solvent was evaporated in vacuo. The crude product was purified by column chromatography (silica gel, hexane/ethyl acetate 4:1) to give the pure compound as colorless oil (4.0 g, 12.04 mmol, 92%).

^{1}H-NMR (400 MHz, $CDCl_3$) δ = 7.78 (d, J = 8.3, 2H), 7.32 (d, J = 8.0, 2H), 4.14 (t, J = 4.8, 2H), 3.67 (t, J = 4.8, 2H), 3.61 3.53 (m, 8H), 3.49 (q, J = 7.0, 2H), 2.42 (s, 3H), 1.18 (t, J = 7.0, 3H).

^{13}C-NMR (100 MHz, $CDCl_3$) δ = 144.75, 132.99, 129.78, 127.94, 70.71, 70.67, 70.49, 69.75, 69.22, 68.63, 66.58, 21.60, 15.12.

4-(2-(2-(2-ethoxyethoxy)ethoxy)ethoxy) benzaldehyde: [27]

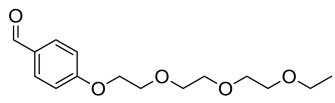

A three-necked, 250 mL round-bottom flask was charged with *p*-hydroxybenzaldehyde (1.55 g, 12.69 mmol), 2-[2-(2-ethoxyethoxy) ethoxy]ethyl *p*-tosylate (4.78 g, 14.38 mmol), K_2CO_3 (5.3 g, 38.4 mmol) and DMF (60 mL). The reaction mixture was stirred overnight at 90 °C. After cooling, the crude reaction mixture was poured into water (100 mL, pH = 2) in a 250 mL Erlenmeyer flask and extracted with dichloromethane. The organic layer was washed subsequently with water (3×25 mL) and brine (1×25 mL) and dried over Na_2SO_4. The solvent was evaporated in vacuo. The crude product was purified by column chromatography (silica gel, hexane/ethyl acetate 4:1) to give pure compound as light yellow oil (3.0 g, 10.64 mmol, 83%).
^{1}H-NMR (400 MHz, $CDCl_3$) δ = 7.80 (d, J = 8.7, 2H), 6.99 (d, J = 8.7, 2H), 4.19 (t, J = 4, 2H), 3.87 (t, J = 4, 2H), 3.71 (m, 3.4, 2H), 3.68 3.60 (m, 4H), 3.56 (m, 2H), 3.49 (q, J = 7.0, 2H), 1.18 (t, J = 7.0, 3H).

PTEG-1:

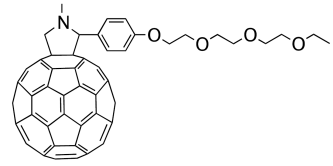

An oven-dried three-necked, 250 mL round-bottom flask was charged with C_{60} (1.08 g, 1.5 mmol), 4-(2-(2-(2-ethoxyethoxy)ethoxy)ethoxy) benzaldehyde (452 mg, 1.6 mmol), sarcosine (435 mg, 4.9 mmol) and o-dichlorobenzene (100 mL). The reaction mixture was stirred under N_2 at 90 °C for 72 h. The mixture was concentrated in vacuo to ∼15 mL, and the crude residue was purified by column chromatography (Silica gel; toluene/ethyl acetate 4:1) to afford the pure compound as a brown solid. The product was re-dissolved in 7 mL of chlorobenzene, precipitated with MeOH, washed repeatedly with MeOH and pentane, and dried in vacuo at 50 °C. This procedure gave 600 mg (0.58 mmol, 39%) of PTEG-1.
^{1}H-NMR (400 MHz, $CDCl_3$) δ = 7.69 (br s, 2H), 6.96 (d, J = 8.6, 2H), 4.97 (d, J = 9.4, 1H), 4.87 (s, 1H), 4.23 (d, J = 9.4, 1H), 4.13 (t, J= 5.0, 2H), 3.84 (t, J= 5.0, 2H), 3.73-3.71 (m, 2H), 3.65-3.63 (m, 4H), 3.60 3.55 (m, 2H), 3.51 (q, J = 7.0, 2H), 2.78 (s, 3H), 1.19 (t, J = 7.0, 3H).
^{13}C-NMR (100 MHz, $CDCl_3$) δ = 158.80, 156.36, 154.09, 153.63, 153.61, 147.29, 147.27, 146.77, 146.51, 146.32, 146.29, 146.24, 146.19, 146.13, 146.11, 146.07, 145.92, 145.90, 145.76, 145.52, 145.47,

145.44, 145.31, 145.29, 145.25, 145.21, 145.12, 144.68, 144.61, 144.37, 143.12, 142.96, 142.65, 142.56, 142.53, 142.52, 142.27, 142.24, 142.14, 142.10, 142.06, 142.01, 142.00, 141.94, 141.82, 141.66, 141.52, 140.13, 140.09, 139.88, 139.58, 136.75, 136.54, 135.78, 135.76, 130.42, 129.09, 114.65, 83.14, 77.22, 70.82, 70.70, 70.63, 69.97, 69.80, 69.73, 68.95, 67.33, 66.63, 39.99, 15.18.

IR (cm^{-1}): 2848, 1609, 1509, 1309, 1259, 1225, 1174, 1126, 1103, 846, 600, 573, 551, 526.

mass m/z: Calcd for $C_{77}H_{27}NO_4$: 1029.2. Found: 1029.8

Anal. Calcd. For $C_{77}H_{27}NO_4$: C, 88.60; H, 2.62; N, 1.36. Found : C, 88.93; H, 2.52; N, 1.41

3,5-bis (2-(2-(2-ethoxyethoxy)ethoxy)ethoxy) benzaldehyde:

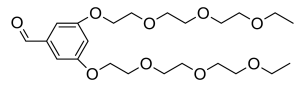

A three-necked, 50 mL round-bottom flask was charged with 3,5-dihydroxybenzaldehyde (500 mg, 3.63 mmol),2-[2-(2-ethoxyethoxy)ethoxy]ethyl *p*-tosylate (2.85 g, 8.58 mmol), K_2CO_3 (1.6 g, 11.58 mmol), and DMF (25 mL). The reaction mixture was stirred over night at 90 °C. After cooling, the crude reaction mixture was poured into water (100 mL, pH = 2) in a 250 mL Erlenmeyer flask and extracted with dichloromethane. The organic layer was washed subsequently with water (3×25 mL) and brine (1×25 mL) and dried over Na_2SO_4. The solvent was evaporated in vacuo. The crude product was purified by column chromatography (silica gel, dichloromethane/ ethyl acetate 3:1) to give pure compound as colorless oil (1.3 g, 2.83 mmol, 78%).

^{1}H-NMR (400 MHz, $CDCl_3$) δ = 9.83 (s, 1H), 6.97 (d, J = 2.3, 2H), 6.71 (t, J = 2.3, 1H), 4.11 (t, J = 4.0, 4H), 3.82 (t, J = 4, 4H), 3.70 3.66 (m, 4H), 3.65 3.58 (m, 8H), 3.54 (m, 4H), 3.47 (q, J = 7.0, 4H), 1.15 (t, J = 8.0, 6H).

^{13}C-NMR (100 MHz, $CDCl_3$) δ = 191.74, 160.34, 138.24, 108.22, 107.91, 70.80, 70.67, 70.59, 69.76, 69.48, 67.79, 66.55, 15.11.

PTEG-2:

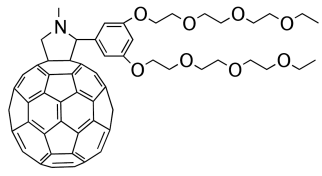

A three-necked, 250 mL round-bottom flask was charged with C_{60} (720 mg, 1.0 mmol), 3,5-bis(2-(2-(2-ethoxyethoxy)ethoxy) ethoxy) benzaldehyde (458 mg, 1mmol), sarcosine (270 mg, 3.0 mmol) and o-dichlorobenzene (100 mL). The reaction mixture was stirred under N2 at 90 °C for 72 h. The reaction mix-

ture was concentrated in vacuo to $\sim$ 15 mL, and the crude residue was purified by column chromatography (silica gel; chloroform/ethyl acetate 3:2) to afford the pure compound as a brown solid. The product was re-dissolved in 7 mL of chlorobenzene, precipitated with MeOH, washed repeatedly with MeOH and pentane, and dried in vacuo at 50 °C. This gave 267 mg (0.22 mmol, 32%) of PTEG-2.

^{1}H-NMR (400 MHz, $CDCl_3$) δ = 6.99 (br, 2H), 6.45 (t, J = 2.1, 1H), 4.95 (d, J = 9.4, 1H), 4.81 (s, 1H), 4.23 (d, J = 9.4, 1H), 4.10 (m, 4H), 3.82 (t, J = 4.9, 4H), 3.74 3.60 (m, 12H), 3.58 (m, 4H), 3.51 (q, J = 7.0, 4H), 2.80 (s, 3H), 1.19 (t, J = 7.0, 6H).

^{13}C-NMR (100 MHz, $CDCl_3$) δ = 158.91, 155.11, 153.06, 152.57, 152.40, 146.27, 145.95, 145.41, 145.28, 145.24, 145.19, 145.12, 145.08, 145.07, 145.05, 144.94, 144.91, 144.74, 144.52, 144.50, 144.45, 144.30, 144.25,144.23, 144.22, 144.21, 144.12, 143.67, 143.59, 143.36, 143.35, 142.11, 141.94, 141.65, 141.54, 141.20, 141.17, 141.13, 141.10, 141.01, 140.91, 140.78, 140.65, 140.59, 139.14, 139.09, 138.83, 138.58, 138.22, 135.56, 135.46, 134.74, 134.69, 101.01, 82.60, 76.20, 75.90, 69.80, 69.68, 69.58, 68.90, 68.79, 68.56, 68.02, 66.52, 65.62, 39.04, 14.17.

IR (cm^{-1}): 2861, 1591, 1443, 1347, 1330, 1293, 1103, 1066, 938, 848, 766, 746, 755, 726, 690, 597, 573, 552, 526.

mass m/z: Calcd for $C_{85}H_{43}NO_8$: 1205.3. Found: 1205.8

Anal. Calcd. For $C_{85}H_{43}NO_8$: C, 84.56; H, 3.56; N, 1.16. Found : C, 83.25; H, 3.63; N, 1.24.

3.9.2 Device fabrication

Commercially available glass substrates patterned with indium tin oxide (ITO) in four different dimensions were used to function as bottom electrode for capacitors. The cleaning of substrates was performed by scrubbing with soap/water solution, rinsing with de-ionized water, sonication in acetone and isopropyl alcohol followed by oven drying and UV-ozone treatment. Poly(3,4-ethylenedioxythiophene):poly(styrenesulfonate) (PEDOT:PSS; VP AI4083, H.C. Starck) was spin cast from an aqueous suspension in ambient condition and oven-dried at 140 °C for 10 minutes. All films were spun from $CHCl_3$ under an inert, nitrogen atmosphere. Metallic contacts and LiF were deposited at a pressure of $\sim 10^{-6}$ mbar by thermal evaporation.

3.9.3 Device characterization

Impedance spectroscopy was performed in the range of 10 Hz to 10 MHz using a Solartron 1260 impedance gain-phase analyzer with an AC drive voltage of 10 mV. Current-voltage characterization was conducted with Keithley 2400 source meter. The stability of measurements was established by carrying the tests under inert, nitrogen atmosphere at a stable temperature (295 K) in the dark. Film thicknesses were obtained using a Dektak 6M Stylus Profiler and, in cases the films were too soft for the tip of the profiler, these thicknesses were verified by AFM profile.

Bibliography

[1] E. L. Mertz and L. I. Krishtalik, "Low dielectric response in enzyme active site", *Proceedings of the National Academy of Sciences* **97**(5), pp. 2081–2086 (2000).

[2] J. P. Roth and J. P. Klinman, "Catalysis of electron transfer during activation of O_2 by the flavoprotein glucose oxidase", *Proceedings of the National Academy of Sciences* **100**(1), pp. 62–67 (2003).

[3] M. Maroncelli, J. Macinnis, and G. R. Fleming, "Polar solvent dynamics and electron-transfer reactions", *Science* **243**(4899), pp. 1674–1681 (1989).

[4] C. Hagleitner, A. Hierlemann, D. Lange, A. Kummer, N. Kerness, O. Brand, and H. Baltes, "Smart single-chip gas sensor microsystem", *Nature* **414**(6861), pp. 293–296 (2001).

[5] S. C. Mannsfeld, B. C. Tee, R. M. Stoltenberg, C. V. H. Chen, S. Barman, B. V. Muir, A. N. Sokolov, C. Reese, and Z. Bao, "Highly sensitive flexible pressure sensors with microstructured rubber dielectric layers", *Nature materials* **9**(10), pp. 859–864 (2010).

[6] A. K. M. Newaz, Y. S. Puzyrev, B. Wang, S. T. Pantelides, and K. I. Bolotin, "Probing charge scattering mechanisms in suspended graphene by varying its dielectric environment", *Nature Communications* **3** (2012).

[7] R. P. Ortiz, A. Facchetti, and T. J. Marks, "High-k organic, inorganic, and hybrid dielectrics for low-voltage organic field-effect transistors", *Chemical reviews* **110**(1), pp. 205–239 (2010).

[8] M.-H. Yoon, C. Kim, A. Facchetti, and T. J. Marks, "Gate dielectric chemical structure-organic field-effect transistor performance correlations for electron, hole, and ambipolar

organic semiconductors", *Journal of the American Chemical Society* **128**(39), pp. 12851–12869 (2006).

[9] H. Klauk, U. Zschieschang, J. Pflaum, and M. Halik, "Ultralow-power organic complementary circuits", *Nature* **445**(7129), pp. 745–748 (2007).

[10] S. A. DiBenedetto, A. Facchetti, M. A. Ratner, and T. J. Marks, "Molecular self-assembled monolayers and multilayers for organic and unconventional inorganic thin-film transistor applications", *Advanced materials* **21**(14-15), pp. 1407–1433 (2009).

[11] P. J. Hotchkiss, H. Li, P. B. Paramonov, S. A. Paniagua, S. C. Jones, N. R. Armstrong, J.-L. Brdas, and S. R. Marder, "Modification of the surface properties of indium tin oxide with benzylphosphonic acids: a joint experimental and theoretical study", *Advanced Materials* **21**(44), pp. 4496–4501 (2009).

[12] S. D. Baranovskii, M. Wiemer, A. V. Nenashev, F. Jansson, and F. Gebhard, "Calculating the efficiency of exciton dissociation at the interface between a conjugated polymer and an electron acceptor", *The Journal of Physical Chemistry Letters* **3**(9), pp. 1214–1221 (2012).

[13] S. Y. Leblebici, T. L. Chen, P. Olalde-Velasco, W. Yang, and B. Ma, "Reducing exciton binding energy by increasing thin film permittivity: an effective approach to enhance exciton separation efficiency in organic solar cells", *ACS applied materials & interfaces* **5**(20), pp. 10105–10110 (2013).

[14] X. Liu, K. S. Jeong, B. P. Williams, K. Vakhshouri, C. Guo, K. Han, E. D. Gomez, Q. Wang, and J. B. Asbury, "Tuning the dielectric properties of organic semiconductors via salt doping", *The Journal of Physical Chemistry B* **117**, pp. 15866–15874 (2013).

[15] N. Camaioni and R. Po, "Pushing the envelope of the intrinsic limitation of organic solar cells", *The Journal of Physical Chemistry Letters* **4**(11), pp. 1821–1828 (2013).

[16] L. J. A. Koster, S. E. Shaheen, and J. C. Hummelen, "Pathways to a new efficiency regime for organic solar cells", *Advanced Energy Materials* **2**(10), pp. 1246–1253 (2012).

[17] M. Breselge, I. Van Severen, L. Lutsen, P. Adriaensens, J. Manca, D. Vanderzande, and T. Cleij, "Comparison of the electrical characteristics of four 2, 5-substituted poly (*p*-phenylene vinylene) derivatives with different side chains", *Thin solid films* **511**, pp. 328–332 (2006).

[18] M. Lenes, F. B. Kooistra, J. C. Hummelen, I. Van Severen, L. Lutsen, D. Vanderzande, T. J. Cleij, and P. W. M. Blom, "Charge dissociation in polymer: fullerene bulk heterojunction solar cells with enhanced permittivity", *Journal of Applied Physics* **104**(11), pp. 114517 (2008).

[19] D. F. Kronholm, J. C. Hummelen, A. B. Sieval, and P. Van't Hof, "Blends of fullerene derivatives, and uses thereof in electronic devices" (2013), US Patent 8,076,050.

[20] R. J. Sengwa, "Solvent effects on microwave dielectric relaxation in poly (ethylene glycols)", *Polymer international* **45**(1), pp. 43–46 (1998).

[21] R. J. Sengwa, K. Kaur, and R. Chaudhary, "Dielectric properties of low molecular weight poly (ethylene glycol) s", *Polymer international* **49**(6), pp. 599–608 (2000).

[22] M. F. Guest, I. J. Bush, H. J. Van Dam, P. Sherwood, J. M. Thomas, J. H. Van Lenthe, R. W. Havenith, and J. Kendrick, "The GAMESS-UK electronic structure package: algorithms, developments and applications", *Molecular Physics* **103**(6-8), pp. 719–747 (2005).

[23] F. Jensen, *Introduction to computational chemistry*, John Wiley & Sons (2007).

[24] M. Prato and M. Maggini, "Fulleropyrrolidines: A family of full-fledged fullerene derivatives", *Accounts of chemical research* **31**(9), pp. 519–526 (1998).

[25] M. A. Lampert and P. Mark, *Current Injection in Solids* volume 10, Academic Press New York (1970).

[26] A. Alliband, F. A. Meece, C. Jayasinghe, and D. H. Burns, "Synthesis and characterization of picket porphyrin receptors that bind phosphatidylglycerol, an anionic phospholipid found in bacterial membranes", *The Journal of organic chemistry* **78**(2), pp. 356–362 (2013).

[27] C.-L. Liu, Y. Chen, D. P. Shelar, C. Li, G. Cheng, and W.-F. Fu, "Bodipy dyes bearing oligo (ethylene glycol) groups on the meso-phenyl ring: tuneable solid-state photoluminescence and highly efficient OLEDs", *Journal of Materials Chemistry C* **2**(28), pp. 5471–5478 (2014).